Nuclear Physics B91 (1975) 12–32

NEW DATA ON $K^-p \to K^-p$ and $\bar{K}^0n$ AND A PARTIAL-WAVE ANALYSIS BETWEEN 1840 AND 2234 MeV CENTER OF MASS ENERGY

R.J. HEMINGWAY, J. EADES, D.M. HARMSEN[+] and J.O. PETERSEN
CERN, Geneva

A. PUTZER
Institut für Hochenergiephysik der Universität Heidelberg

C. KIESLING, D.E. PLANE[++] and W. WITTEK
Max-Planck-Institut für Physik und Astrophysik, München

Received 30 December 1974

The angular distributions of the reactions $K^-p \to K^-p$ and $K^-p \to \bar{K}^0n$ have been measured at 23 incident K^- momenta between 1.136 and 1.798 GeV/c using the bubble chamber technique. These data, together with other published data on the same reactions, including K^-p polarisations, $\bar{K}N$ total cross sections, and measurements of $\mathrm{Re}\, f(0)/\mathrm{Im}\, f(0)$, have been analysed in terms of partial-wave amplitudes. Resonance behaviour is confirmed for the P_{03} partial wave at 1890 MeV. The resonance parameters of the $F_{15}(1915)$, $F_{17}(2030)$ and $G_{07}(2100)$ have been redetermined. No evidence has been found for new resonances coupling significantly to $\bar{K}N$ in the energy region explored.

1. Introduction

This paper reports results of a series of bubble chamber experiments to study the $\bar{K}N$ interaction over the range of incident K^- lab momenta 1.136 to 1.798 GeV/c. These experiments, of which the data analysis details are to be published separately [1, 2], continue to higher energies the detailed study of the $\bar{K}N$ interaction [3]. In particular, we deal with the $\bar{K}N$ final state, *viz.* the reactions

$$K^-p \to K^-p, \tag{1}$$

$$K^-p \to \bar{K}^0n. \tag{2}$$

+ Present address: Institut für Systemtechnik und Innovationsforschung, Karlsruhe.
++ Now at CERN.

The differential cross sections have been measured at intervals of approximately 30 MeV/c. The coefficients of the Legendre polynomial expansion are presented in tabular form.

The new data from these experiments have been combined with the available data from other experiments, thus allowing an energy-dependent partial-wave analysis within the incident momentum range 1.1 – 2.0 GeV/c, corresponding to a centre of mass energy range 1840 – 2234 MeV. The statistical content of the combined data increases by a factor of 4 that which was used in a previous analysis of the $\bar{K}N$ system in the c.m. energy range 1915 – 2168 MeV [4].

In addition to a better determination of the parameters of the established resonances $F_{17}(2030)$ and $G_{07}(2100)$ which dominate the energy region investigated we observe a significant coupling of the $F_{15}(1915)$ resonance to $\bar{K}N$ and confirm the resonance behaviour for P_{03} at 1890 MeV [5] *. A good fit to the experimental data can be obtained without the addition of further resonances.

2. Discussion of the data

2.1. New data from this experiment

Reactions (1) and (2) have been analysed at 13 momenta between 1.136 and 1.434 GeV/c from 300 000 pictures taken in the 81 cm hydrogen bubble chamber at CERN, and at 10 additional momenta between 1.424 and 1.798 GeV/c from 400 000 pictures taken in the 2 m hydrogen bubble chamber at CERN. The experimental details, the treatment of the biases, and the technique of cross-section normalisation are not presented here. They are to be published together with a general discussion of all reactions investigated in the experiment [1, 2].

The differential cross sections for both reactions (1) and (2) in the c.m. system have been fitted to a Legendre polynomial expansion of the type:

$$\frac{d\sigma}{d\Omega} = \lambda\!\!\!^{-2} \sum_{n=0}^{m} A_n P_n (\cos\theta), \tag{3}$$

where $1/\lambda\!\!\!^{-} = k$ is the c.m. momentum, θ is the meson scattering angle in the c.m. system and P_n is the Legendre polynomial of order n. Table 1 gives the A_n coefficients for both reactions at each of the 23 momenta **. The coefficients are displayed in fig. 1 together with data from other experiments (see 2.2). Apart from

* We use throughout the conventional spectroscopic notation $L_{I,2J}$ to denote a partial wave with orbital angular momentum L, isospin I and total angular momentum J.

** Five momenta of reaction (1) have been measured independently and partially published [6]. All coefficients are given here for completeness.

Table 1

The A_n coefficients of the Legendre expansion $d\sigma/d\Omega = \lambda^2 \Sigma A_n P_n(\cos\theta)$ of the reactions $K^- p \to K^- p$ and $K^- p \to \bar{K}^0 n$ at each of the 23 momenta of this experiment.

K^- momentum [GeV/c]	$K^- p \to K^- p$										$K^- p \to \bar{K}^0 n$									
	A_0	A_1	A_2	A_3	A_4	A_5	A_6	A_7	A_8	A_9	A_0	A_1	A_2	A_3	A_4	A_5	A_6	A_7	A_8	A_9
1.136	1.061 0.026	1.715 0.058	2.210 0.074	1.608 0.082	0.903 0.087	0.489 0.084	-0.070 0.083				0.302 0.023	-0.062 0.040	0.445 0.051	-0.142 0.064	0.371 0.069	-0.323 0.075	0.227 0.082	-0.105 0.089		
1.159	1.062 0.022	1.717 0.052	2.153 0.066	1.560 0.073	0.837 0.078	0.402 0.074	0.007 0.071				0.245 0.019	-0.079 0.032	0.314 0.042	-0.096 0.051	0.230 0.057	-0.322 0.061	0.129 0.066	-0.004 0.071		
1.178	1.040 0.024	1.667 0.054	2.002 0.071	1.399 0.079	0.712 0.084	0.483 0.081	0.076 0.079				0.272 0.026	-0.018 0.043	0.305 0.056	-0.001 0.068	0.233 0.075	-0.207 0.079	0.089 0.087	0.093 0.097		
1.200	0.925 0.021	1.559 0.049	1.886 0.061	1.343 0.068	0.705 0.072	0.352 0.070	-0.016 0.069				0.218 0.021	-0.102 0.037	0.268 0.048	-0.092 0.059	0.233 0.063	-0.311 0.068	0.072 0.080	0.042 0.085		
1.232	0.986 0.023	1.658 0.051	1.930 0.065	1.315 0.072	0.744 0.078	0.404 0.075	-0.056 0.068				0.184 0.018	-0.063 0.033	0.245 0.042	-0.058 0.055	0.180 0.060	-0.351 0.065	0.174 0.072	-0.098 0.077		
1.252	0.920 0.022	1.544 0.051	1.852 0.064	1.322 0.072	0.750 0.076	0.347 0.073	0.059 0.069				0.145 0.017	-0.100 0.030	0.182 0.038	-0.100 0.046	0.098 0.052	-0.143 0.060	-0.007 0.070	0.003 0.074		
1.275	0.908 0.021	1.525 0.047	1.866 0.059	1.385 0.066	0.738 0.068	0.415 0.068	-0.092 0.066				0.158 0.016	-0.112 0.029	0.239 0.036	-0.231 0.046	0.171 0.052	-0.274 0.055	0.164 0.062	-0.033 0.069		
1.295	0.941 0.023	1.620 0.051	1.924 0.062	1.419 0.066	0.707 0.071	0.335 0.072	-0.032 0.071				0.160 0.019	-0.086 0.037	0.279 0.042	-0.147 0.060	0.091 0.067	-0.280 0.071	0.240 0.081	-0.031 0.088		
1.305	0.885 0.038	1.525 0.084	1.784 0.116	1.288 0.135	0.624 0.148	0.287 0.153	-0.047 0.145	0.107 0.117	-0.031 0.090		0.179 0.014	-0.061 0.026	0.260 0.031	-0.147 0.040	0.071 0.043	-0.226 0.047	0.117 0.050	-0.036 0.055		
1.336	0.873 0.037	1.469 0.081	1.788 0.112	1.312 0.131	0.606 0.142	0.172 0.147	-0.249 0.138	-0.059 0.112	-0.108 0.087		0.164 0.014	-0.026 0.024	0.222 0.031	-0.142 0.042	0.097 0.047	-0.150 0.052	0.249 0.055	-0.078 0.060		
1.367	0.830 0.035	1.501 0.080	1.967 0.114	1.448 0.130	0.688 0.140	0.530 0.142	0.161 0.130	0.215 0.100	0.075 0.079		0.155 0.013	-0.042 0.024	0.183 0.030	-0.156 0.038	0.113 0.041	-0.076 0.045	0.128 0.048	-0.053 0.052		
1.396	0.862 0.036	1.588 0.084	2.106 0.120	1.767 0.137	1.268 0.146	0.756 0.144	0.263 0.131	0.279 0.100	0.054 0.078		0.146 0.014	0.009 0.028	0.218 0.036	-0.157 0.047	0.140 0.053	-0.178 0.054	0.250 0.061	-0.183 0.067		
1.424	0.880 0.045	1.531 0.091	2.072 0.127	1.730 0.129	1.198 0.126	0.681 0.124	0.270 0.119	0.209 0.109	0.089 0.085	-0.079 0.060	0.175 0.015	0.067 0.026	0.191 0.033	-0.150 0.042	0.064 0.041	-0.040 0.048	0.165 0.055	-0.095 0.057	-0.127 0.051	-0.099 0.061
1.434	0.808 0.036	1.478 0.084	2.112 0.122	1.756 0.140	1.151 0.144	0.754 0.148	0.231 0.134	0.275 0.102	-0.049 0.080		0.171 0.014	0.062 0.025	0.186 0.031	-0.122 0.040	0.073 0.044	-0.088 0.047	0.153 0.051	-0.119 0.056		
1.478	0.784 0.032	1.546 0.068	2.204 0.098	2.014 0.101	1.594 0.098	1.103 0.092	0.646 0.084	0.556 0.074	0.169 0.054	0.127 0.043	0.148 0.008	0.101 0.013	0.113 0.016	-0.116 0.019	-0.023 0.021	-0.079 0.025	0.110 0.025	-0.134 0.028	-0.043 0.028	0.034 0.031
1.519	0.836 0.038	1.709 0.083	2.401 0.119	2.220 0.121	1.767 0.115	1.144 0.105	0.581 0.093	0.430 0.081	0.076 0.059	0.075 0.046	0.144 0.009	0.159 0.016	0.159 0.019	-0.046 0.025	0.072 0.025	-0.044 0.031	0.081 0.031	-0.143 0.035	0.022 0.034	-0.012 0.034
1.567	0.872 0.035	1.824 0.076	2.610 0.110	2.571 0.115	2.140 0.108	1.433 0.093	0.815 0.079	0.518 0.066	0.129 0.049	0.037 0.038	0.196 0.008	0.193 0.013	0.169 0.016	0.068 0.018	0.109 0.021	0.009 0.024	0.030 0.024	-0.148 0.024	-0.006 0.027	0.012 0.027
1.608	0.914 0.039	1.970 0.048	2.816 0.136	2.835 0.134	2.377 0.126	1.666 0.110	1.008 0.093	0.652 0.077	0.140 0.055	0.120 0.043	0.187 0.008	0.146 0.013	0.146 0.016	0.073 0.018	0.082 0.021	0.006 0.024	0.024 0.024	-0.143 0.028	0.021 0.030	0.012 0.030
1.651	0.901 0.037	2.032 0.085	2.818 0.120	2.861 0.127	2.378 0.117	1.628 0.099	0.980 0.082	0.517 0.067	0.207 0.050	0.062 0.037	0.197 0.008	0.206 0.014	0.170 0.018	0.124 0.022	0.127 0.022	0.091 0.024	0.094 0.027	-0.119 0.031	0.033 0.030	0.024 0.030
1.691	1.017 0.039	2.337 0.093	3.190 0.129	3.266 0.137	2.699 0.126	1.828 0.106	1.054 0.087	0.567 0.071	0.188 0.053	0.059 0.039	0.163 0.009	0.181 0.014	0.154 0.016	0.086 0.019	0.080 0.022	0.043 0.025	-0.009 0.025	-0.158 0.028	-0.022 0.028	-0.015 0.028
1.726	0.977 0.043	2.251 0.101	3.042 0.139	3.076 0.147	2.494 0.136	1.646 0.117	0.954 0.101	0.450 0.086	0.127 0.064	0.037 0.051	0.140 0.015	0.177 0.025	0.173 0.031	0.122 0.038	0.105 0.044	0.088 0.048	0.041 0.051	-0.149 0.055	0.031 0.054	0.112 0.055
1.763	1.077 0.046	2.474 0.107	3.379 0.149	3.378 0.156	2.778 0.143	1.752 0.120	0.865 0.099	0.338 0.085	-0.021 0.063	-0.001 0.051	0.193 0.014	0.268 0.026	0.268 0.035	0.227 0.038	0.141 0.043	0.132 0.049	0.009 0.052	-0.153 0.055	-0.006 0.055	-0.031 0.055
1.798	1.130 0.065	2.594 0.153	3.523 0.211	3.484 0.219	2.843 0.200	1.757 0.168	0.890 0.142	0.299 0.121	-0.115 0.093	-0.042 0.073	0.169 0.015	0.213 0.030	0.282 0.043	0.253 0.045	0.185 0.051	0.084 0.056	-0.013 0.059	-0.075 0.063	0.031 0.059	-0.013 0.063

discrepancies in normalisation among some older experiments, the agreement is generally good. The use of all data in the subsequent analysis thus poses no special problem. We remark that the non-zero values of the A_8 coefficient for reaction (1) necessitate an analysis involving partial waves up to at least G_{19}.

2.2. Data from other experiments

To complement the data from this experiment, we have used the following data over the incident momentum range 1.1 – 2.0 GeV/c:

(a) Differential cross sections of $K^- p \to K^- p$ at 63 momenta [7]

(b) Differential cross sections of $K^- p \to \bar{K}^0 n$ at 40 momenta [8]

(c) Partial cross sections of $K^- p \to \bar{K}^0 n$ at 33 momenta [9]

(d) Interpolated $K^- p$ total cross sections and $I = 1$ total cross sections at 97 momenta [10]

(e) Ratio Re/Im of the forward elastic scattering amplitude at 10 momenta [11]

(f) Polarisations of $K^- p \to K^- p$ at 28 momenta [12]

These data are displayed in figs. 1–3. The differential cross section is given in terms of A_n coefficients and the polarisation in terms of B_n coefficients. B_n is defined by

$$|\boldsymbol{P}| \frac{d\sigma}{d\Omega} = \chi^2 \sum_{n=1}^{m'} B_n P_n^1(\cos\theta), \tag{4}$$

where P_n^1 is the associated Legendre polynomial of order n.

For practical reasons the total cross sections have been interpolated to momenta at which other data exists. For the $I = 1$ total cross section we have assigned an error of 0.5 mb to prevent the systematic errors in $K^- d$ total cross-section measurements and the uncertainties in the procedure of extracting the $K^- n$ total cross section [13] from unduly constraining the analysis. For comparison, the $K^- p$ total cross section is measured to within 0.1 mb over most of the c.m. energy range. The values for the ratio Re/Im of the forward elastic scattering amplitude are taken at intervals of ~ 0.1 GeV/c from a dispersion relation calculation [11], which is based in part on recent measurements [14] of Re $f(0)$/Im $f(0)$ at 4-momenta within the energy region investigated in this analysis.

Fig. 4 shows the density of all data used in this analysis. Only above 1.8 GeV/c does the density of information tend to diminish. Expressing the differential cross section and polarisation in terms of A_n and B_n coefficients, the total number of data points is 1602, where 437 are from the present experiment and only ~ 400 are in common with the analysis of [4]. The new data from this experiment amounts to $\sim 25\%$ of the total available data on differential cross sections in the energy range of 1840 to 2234 MeV, but it is based on significantly better statistics.

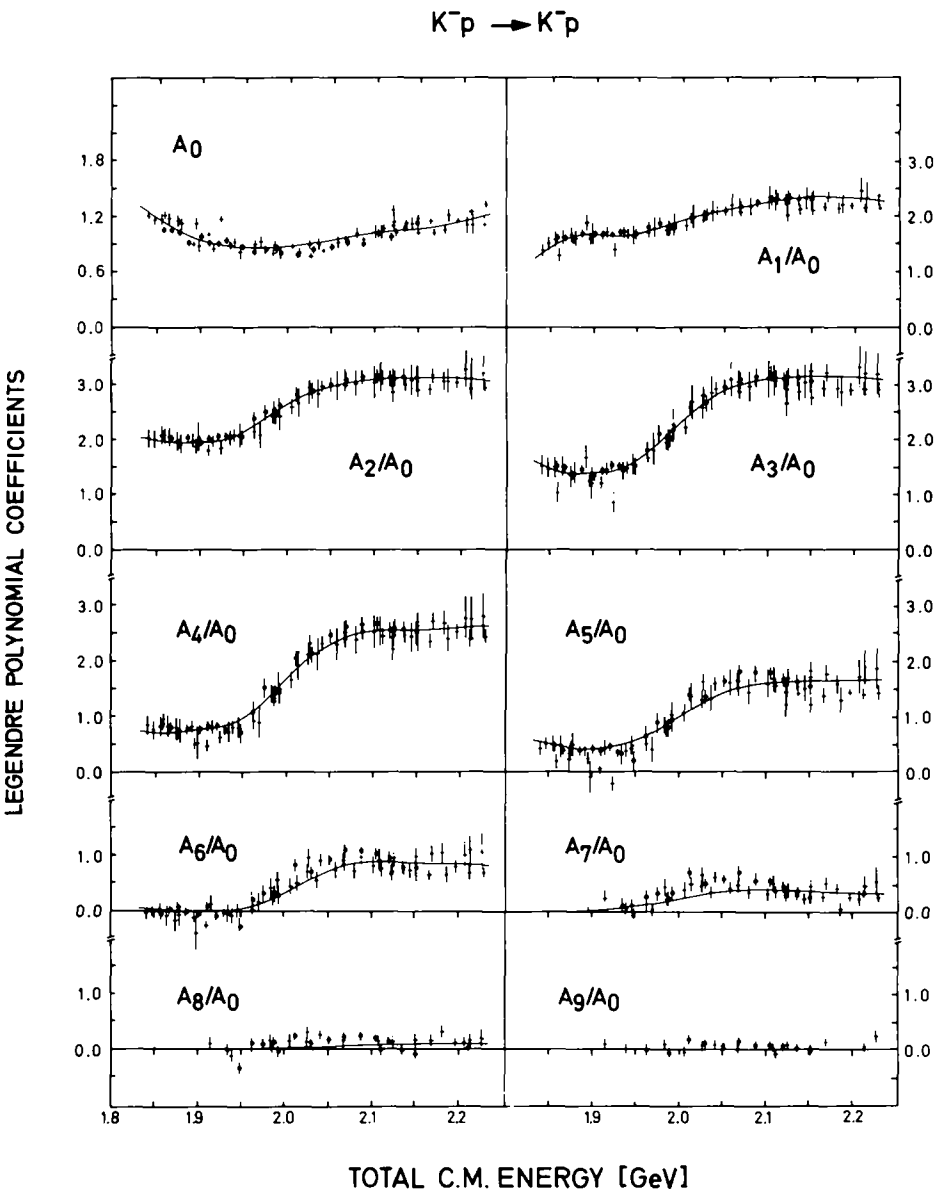

Fig. 1a. The A_n coefficients of the Legendre polynomial expansion $d\sigma/d\Omega = \lambda^2 \Sigma A_n P_n (\cos\theta)$ of the reaction $K^- p \to K^- p$ for all data used in this analysis. The solid circles represent the data from this experiment. The superposed curves represent solution B.

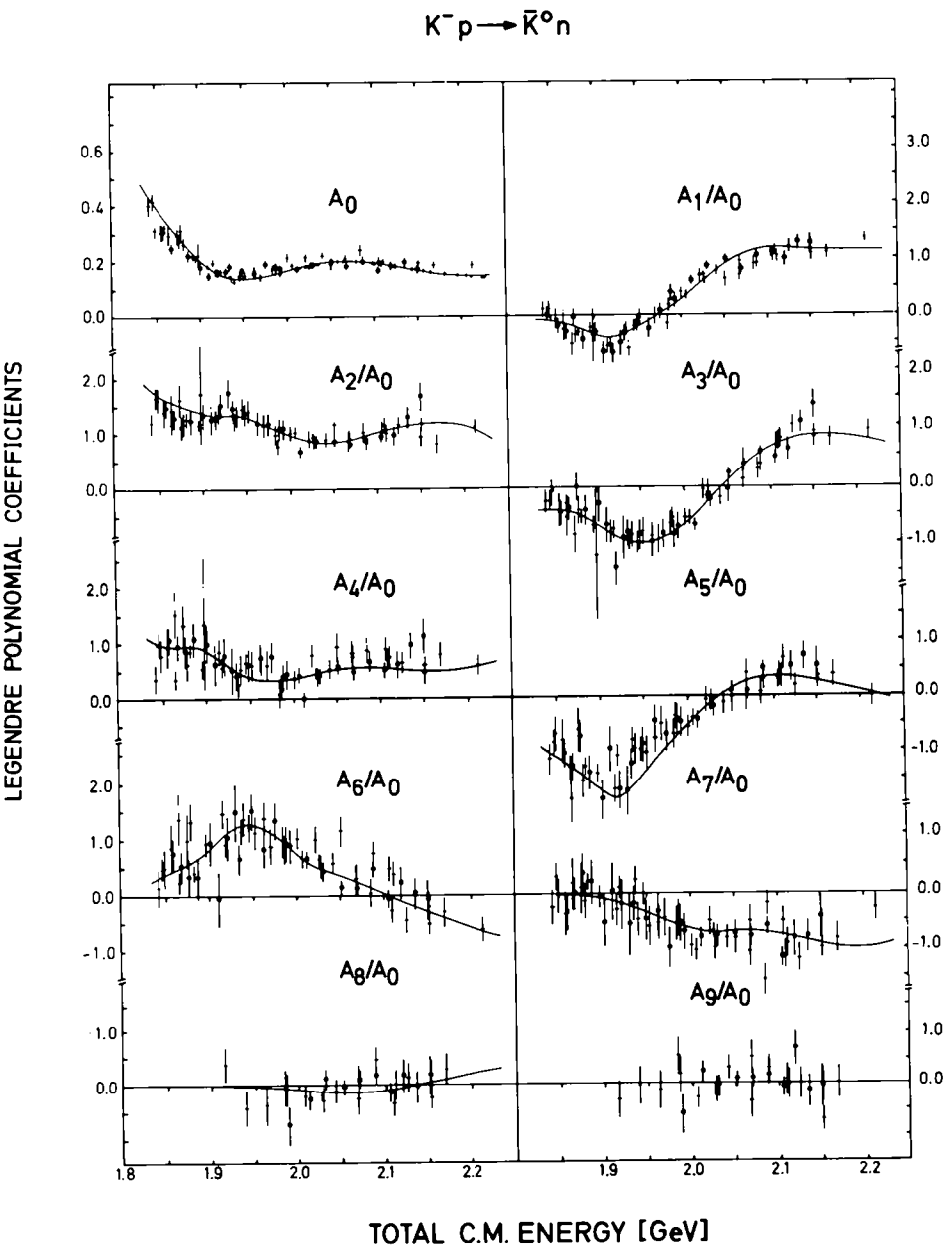

Fig. 1b. The A_n coefficients of the Legendre polynomial expansion $d\sigma/d\Omega = \lambda^2 \Sigma A_n P_n (\cos\theta)$ of the reaction $K^- p \to \bar{K}^0 n$ for all data used in this analysis, including also partial cross-section measurements. The solid circles represent the data from this experiment. The superposed curves represent solution B.

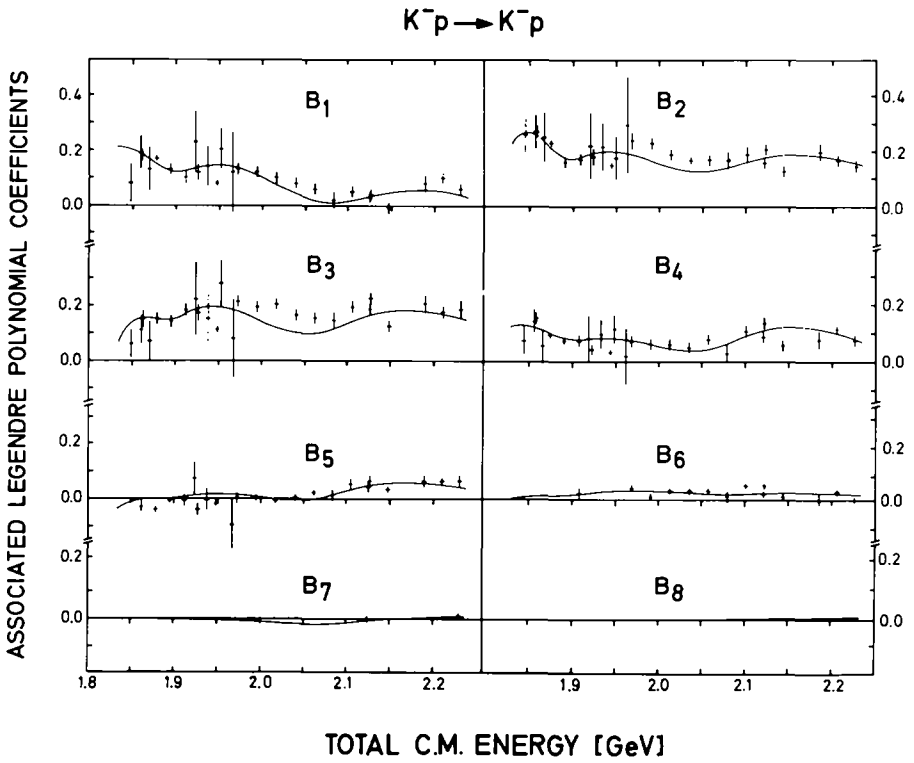

Fig. 2. The B_n coefficients of the associated Legendre polynomial expansion $|P|\, d\sigma/d\Omega = \lambda^2 \Sigma B_n P_n^1(\cos\theta)$ of the reaction $K^-p \to K^-p$ for all data used in this analysis. The superposed curves represent solution B. Although the B_n coefficients were not fitted (polarisation measurements were used directly) they are displayed for convenience.

3. Partial-wave analysis

The amplitude for a given partial wave $L_{I,2J}$ has been parameterised as

$$T = T_B + e^{i\phi} T_R , \tag{5}$$

where T_B is a background amplitude, and T_R is a Breit-Wigner resonance amplitude. The factor $e^{i\phi}$ expresses the well known fact that the resonance amplitude can be rotated in the presence of a background. For T_B a Legendre polynomial expansion has been chosen as a parameterisation sufficiently flexible over the whole energy region:

$$T_B = \sum_{n=0}^{N} a_n P_n(y), \tag{6}$$

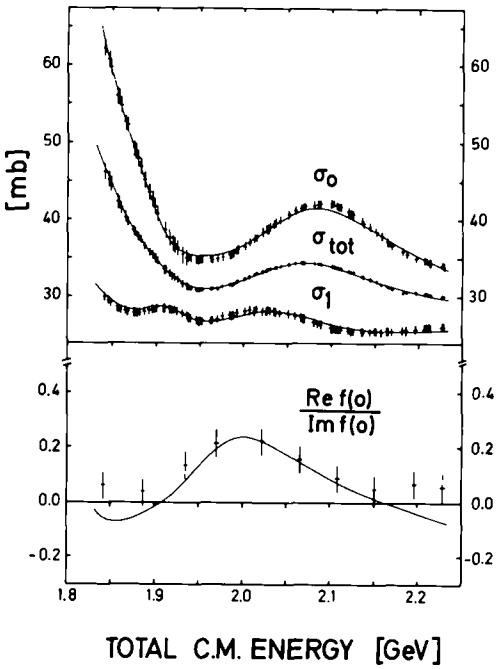

Fig. 3. The $K^- p$ total cross section, its $I = 0$ and $I = 1$ components and values for $\mathrm{Re}\, f(0)/\mathrm{Im}\, f(0)$. The $I = 0$ component of the total cross section has not been used in the fit. The superposed curves represent solution B.

with

$$y = \frac{2E - E_{\max} - E_{\min}}{E_{\max} - E_{\min}} \quad ,$$

$$E_{\min} \leqslant E \leqslant E_{\max}, \qquad \text{i.e.} -1 \leqslant y \leqslant 1,$$

where the a_n are a set of complex parameters, the functions $P_n(y)$ are Legendre polynomials and E is the c.m. energy. For the lower partial waves, with appreciable background amplitudes over the entire energy range, $E_{\min}$ and $E_{\max}$ have been taken as 1794 and 2274 MeV respectively corresponding to the lab momenta 1.0 and 2.1 GeV/c. For the higher partial waves which only start to be significant within the range, $E_{\min}$ is left as a free parameter to be determined by the fit and $E_{\max}$ is fixed at 2274 MeV. In the latter case, the background amplitude is constrained to be zero below and at $E_{\min}$. As to be choices of N, see below.

The resonance amplitude T_R has been parameterised as

$$T_R = \frac{t}{\epsilon - i} \, , \tag{7}$$

where t is the resonant amplitude, $\epsilon = (2/\Gamma(E))\,(E_R - E)$ and

$$\Gamma(E) = \Gamma(E_R)\frac{kB_l(kr)}{k_R B_l(k_R r)} ,$$

with $B_l(kr)$ taken from [15]. In these formulae, E_R is the resonance mass, k_R is the c.m. momentum at the resonance mass, $\Gamma(E_R)$ is the resonance width, $B_l(kr)$ is a centrifugal barrier factor for orbital angular momentum l, and r is the radius of interaction, taken to be 1 fm.

In order to be independent of this specific parameterisation at energies far above the resonance mass E_R where the Breit-Wigner description may no longer be valid, the resonance parameterisation has been kept only up to an energy $E_C = E_R + c\Gamma(E_R)$ (c to be determined by the fit). For $E > E_C$, a pure background amplitude has been assumed such that the total partial wave amplitude is continuous at E_C.

The parameters of the resonance and background amplitudes have been determined by χ^2 fits to the experimental data. As far as the polarisation measurements are concerned, we have chosen to use directly the measured polarisations of reaction (1) rather than the more customary coefficients of the expansion in associated Legendre polynomials. The latter appear to suffer from uncertainties in the normalisation of the elastic cross section and from an incomplete coverage of the full range of scattering angle [12]. Concerning the differential cross sections, we used in the first stage of fitting (basic starting solution) the A_n coefficients because of computer time limitations, whereas the final fits were performed on $d\sigma/d\Omega$. The total number of data points is 2111 (A_n coefficients and differential polarisations) and 4354 (differential cross sections and polarisations) respectively. Fitting the differential cross sections and polarisations directly has the advantage of removing correlations among data points, which are usually not taken into account when coefficients are used.

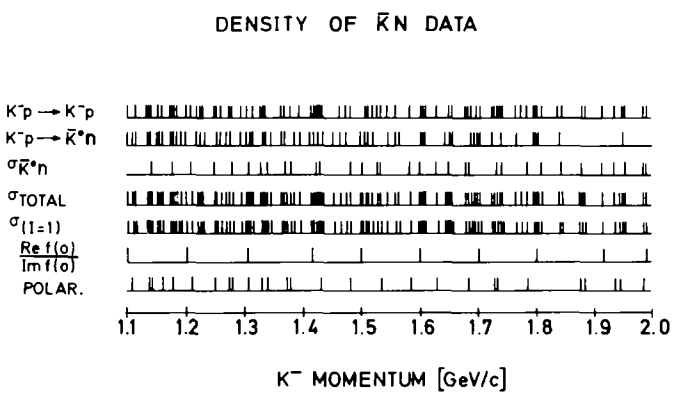

Fig. 4. Distribution of K^- lab momenta of the data used in this analysis.

Table 2
Comparison of fit A (with F_{07} resonance) with fit B (without F_{07} resonance)

		fit A	fit B
total number of data points		4354	4354
number of variable parameters		93	91
total χ^2		6428	6307
χ^2/degree of freedom		1.51	1.48
differential cross sections	data	3323	3323
	χ^2	4817	4790
	χ^2/data p.	1.45	1.44
partial cross sections	data [a]	379	379
total cross sections	χ^2	667	675
Re $f(0)$/Im $f(0)$	χ^2/data p.	1.76	1.78
polarisations	data	652	652
	χ^2	944	842
	χ^2/data p.	1.45	1.29
projection onto A_n coefficients	data	1255	1255
	χ^2	2117	2051
	χ^2/data p.	1.69	1.63
projection onto B_n coefficients	data	143	143
	χ^2	440	443
	χ^2/data p.	3.1	3.1

[a] This number contains 204 data points from σ_{tot}, σ_1, Re/Im, and 175 A_0 coefficients from reactions (1) and (2).

Below the energy range of the present analysis there are three well established resonances, $D_{15}(1765)$, $F_{05}(1815)$ and $D_{05}(1830)$, whose elastic amplitudes are still significant at 1840 MeV. These resonances have been input throughout with parameters fixed at the values given in table 3. An attempt to find a basic starting solution has been carried out imposing the following conditions simultaneously:

(i) The F_{17} and G_{07} amplitudes were taken as resonant with variable parameters,

(ii) The $J = \frac{1}{2}$ amplitudes were described by a fourth order polynomial background,

(iii) The $J = \frac{3}{2}, \frac{5}{2}$ amplitudes were described by a second order polynomial background,

(iv) The amplitudes F_{07}, G_{17}, G_{09} and G_{19} were described by a first order polynomial background.

A large number of random searches was made to find a set of parameters giving a

Table 3
Resonance parameters of fit B

	E_R mass (MeV)	$\Gamma(E_R)$ width (MeV)	t amplitude	ϕ phase (rad)	background
P_{03}	1894 ± 10	107 ± 10	0.24 ± 0.04	1.23	a
D_{05}	[1825]	[105]	[0.08]		a
D_{15}	[1765]	[120]	[0.41]		b
F_{05}	[1820]	[84]	[0.62]		b
F_{15}	1914 ± 10	85 ± 15	0.11 ± 0.04		b
F_{17}	2038 ± 10	172 ± 15	0.18 ± 0.03		
G_{07}	2105 ± 10	241 ± 30	0.31 ± 0.03		

The parameters within square brackets were kept fixed, they were obtained by averaging the values given in [16].

a: background superposed on resonance throughout the energy region, as in eq. (5).

b: background starting at E_C, E_C as defined in the text ($E_C > E_R$).

reasonable fit to the data. It turned out that the maximum order N in eq. (6) required by the data was 2 for all partial waves up to F_{15} and 1 for the higher partial waves. Only one good solution was found, having a χ^2 of 3363 for 2111 data points and 86 parameters (basic starting solution).

Resonances were now added in turn to each partial wave not already parameterised as such. Most resonances suggested by other analyses have been tried and sizable reductions in χ^2 were observed in only three cases – a P_{03} at ~ 1890 MeV, an F_{15} at ~ 1915 MeV, and an F_{07} at ~ 2100 MeV. Retaining these resonances, a complete final fit was now attempted incorporating the binned differential cross sections rather than the A_n coefficients (fit A). Since it appeared that the parameters of the F_{07} were rather unstable, and especially since its resonant amplitude was small, we performed a further fit without the F_{07} resonance (fit B). As can be seen from table 2, the two fits are of comparable quality, which means that the data do not require an F_{07} state around 2100 MeV. The resulting values for the 91 variable parameters of solution B are tabulated in tables 3 and 4. Table 5 gives the corresponding partial wave amplitudes in steps of 20 MeV. The Argand diagrams for the partial waves are shown in fig. 6.

Solution B is represented by the curves in figs. 1–3. Furthermore, fig. 5 displays the measured elastic and charge-exchange differential cross sections from this experiment at three momenta spanning the fitted c.m. energy range together with polarisation data [12] at similar momenta. The superposed curves represent solution B. Although the fit reproduces well the polarisation, this is not the case for the B_n coefficients (see fig. 2). This confirms our previous remark that the B_n coefficients may be unreliable representations of the measured polarisation, if the measurements do not cover the full angular range.

We have calculated the contributions to the χ^2 of the fit from the various energies

Table 4
Background parameters for fit B

	Re a_0	Im a_0	Re a_1	Im a_1	Re a_2	Im a_2	E_{min}	c
S_{01}	0.133	0.529	-0.108	-0.096	-0.080	0.089		
S_{11}	0.037	0.488	-0.082	-0.304	0.078	0.086		
P_{01}	0.092	0.506	0.031	-0.252	0.142	0.153		
P_{11}	0.113	0.413	0.233	0.028	-0.141	0.085		
P_{03}	0.181	0.304	-0.133	0.136	-0.070	-0.037		
P_{13}	0.054	0.193	-0.031	0.173	-0.141	0.052		
D_{03}	0.033	0.184	0.072	0.125	0.037	-0.039		
D_{13}	0.073	0.176	0.013	0.175	-0.168	0.079		
D_{05}	0.117	0.081	0 012	0.081	-0.058	0.012		
D_{15}			0.058	-0.007	-0.025	0.005		1.48
F_{05}			0.004	0.110	0.104	0.001		1.17
F_{15}			0.014	0.140	0.038	0.029		1.09
F_{07}	0.016	0.050	0.027	0.036	-0.027	0.007		
F_{17}								
G_{07}								
G_{17}			0.071	0.065			2.04	
G_{09}			-0.005	0.012			1.95	
G_{19}			0.013	0.020			1.92	

The background amplitudes are parameterised as in eq. (6). The definitions of E_{min} and c are found in the text. Blank entries for a_0 mean that this quantity has not been fitted but calculated from the continuity conditions for the partial-wave amplitudes at E_C or E_{min} (see sect. 3).

over the range 1840–2234 MeV and find no region where the quality of the fit significantly deteriorates. We conclude that no additional structure in the corresponding mass range is required by the data. The errors on the resonance parameters in table 3 indicate the spread of values obtained in the different fits that we have attempted. With the adopted model, these parameters appear to be stable within the stated tolerances.

4. Discussion of results

4.1. Resonance parameters

Fig. 7 displays the resonance parameters for the $P_{03}(1860)$, $G_{07}(2100)$, $F_{15}(1915)$, and $F_{17}(2030)$ resulting from the present analysis together with other existing results obtained either in partial-wave analyses or in fits to total and partial cross sections. The resonances $D_{05}(1830)$, $D_{15}(1765)$, $F_{05}(1815)$ are not displayed in the figure since their parameters have been kept fixed in the fit (see table 3). Due to the limited range of c.m. energy, reliable information on these resonances cannot be obtained in this analysis.

Table 5
The fitted partial-wave amplitudes from fit B at energy intervals of 20 MeV

Total c.m. energy (GeV)	Re S_{01}	Im S_{01}	Re P_{01}	Im P_{01}	Re P_{03}	Im P_{03}	Re D_{03}	Im D_{03}	Re D_{05}	Im D_{05}	Re F_{05}	Im F_{05}	Re F_{07}	Im F_{07}	Re G_{07}	Im G_{07}	Re G_{09}	Im G_{09}
	Re S_{11}	Im S_{11}	Re P_{11}	Im P_{11}	Re P_{13}	Im P_{13}	Re D_{13}	Im D_{13}	Re D_{15}	Im D_{15}	Re F_{15}	Im F_{15}	Re F_{17}	Im F_{17}	Re G_{17}	Im G_{17}	Re G_{19}	Im G_{19}
1.84	0.18	0.56	0.13	0.78	0.19	0.33	-0.11	0.06	0.06	0.08	-0.23	0.53	-0.32	0.02	0.03	0.00	0.0	0.0
	0.14	0.77	-0.14	0.43	0.01	0.03	-0.02	-0.00	-0.20	0.21	0.04	0.02	0.04	0.01	0.0	0.0	0.0	0.0
1.86	0.19	0.57	0.11	0.73	0.14	0.35	-0.09	0.08	0.06	0.08	-0.30	0.38	-0.01	0.03	0.04	0.01	0.0	0.0
	0.12	0.73	-0.10	0.42	0.04	0.05	0.02	0.03	-0.20	0.17	0.05	0.03	0.05	0.01	0.0	0.0	0.0	0.0
1.88	0.19	0.58	0.09	0.69	0.07	0.34	-0.08	0.10	0.06	0.07	-0.31	0.29	-0.00	0.03	0.05	0.01	0.0	0.0
	0.10	0.69	-0.09	0.40	0.06	0.09	0.05	0.05	-0.19	0.14	0.05	0.04	0.05	0.02	0.0	0.0	0.0	0.0
1.90	0.20	0.59	0.07	0.64	0.03	0.28	-0.07	0.12	0.07	0.07	-0.30	0.22	0.00	0.03	0.06	0.01	0.0	0.0
	0.08	0.65	-0.01	0.39	0.08	0.10	0.07	0.08	-0.19	0.12	0.03	0.10	0.06	0.03	0.0	0.0	0.0	0.0
1.92	0.20	0.59	0.05	0.60	0.04	0.23	-0.06	0.13	0.08	0.07	-0.29	0.22	0.01	0.03	0.08	0.02	0.0	0.0
	0.06	0.62	0.03	0.39	0.09	0.12	0.09	0.11	-0.18	0.10	-0.01	0.11	0.07	0.04	0.0	0.0	0.00	0.00
1.94	0.20	0.59	0.04	0.56	0.08	0.20	-0.05	0.15	0.09	0.07	-0.26	0.24	0.01	0.03	0.10	0.03	0.0	0.0
	0.05	0.59	0.06	0.38	0.10	0.14	0.11	0.13	-0.17	0.09	-0.05	0.08	0.08	0.04	0.0	0.0	0.00	0.00
1.96	0.19	0.59	0.03	0.53	0.11	0.20	-0.04	0.16	0.10	0.08	-0.23	0.25	0.02	0.04	0.11	0.05	-0.00	0.00
	0.03	0.55	0.09	0.37	0.11	0.16	0.13	0.15	-0.16	0.09	-0.05	0.06	0.09	0.04	0.0	0.0	0.00	0.00
1.98	0.19	0.59	0.02	0.50	0.13	0.21	-0.03	0.17	0.11	0.08	-0.21	0.26	0.02	0.04	0.13	0.06	-0.00	0.00
	0.02	0.52	0.12	0.37	0.12	0.18	0.14	0.17	-0.14	0.09	-0.05	0.04	0.09	0.11	0.0	0.0	0.00	0.01
2.00	0.19	0.58	0.02	0.47	0.14	0.22	-0.02	0.18	0.11	0.09	-0.19	0.27	0.02	0.04	0.15	0.11	-0.00	0.00
	0.01	0.49	0.15	0.37	0.12	0.19	0.15	0.18	-0.13	0.09	-0.05	0.03	0.07	0.15	0.0	0.0	0.01	0.01
2.02	0.18	0.58	0.02	0.44	0.15	0.24	-0.02	0.20	0.12	0.09	-0.17	0.29	0.01	0.04	0.15	0.16	-0.00	0.01
	0.00	0.46	0.17	0.37	0.12	0.21	0.16	0.20	-0.12	0.08	-0.06	0.04	0.04	0.17	0.0	0.0	0.01	0.01
2.04	0.17	0.57	0.02	0.42	0.15	0.26	-0.01	0.21	0.12	0.10	-0.15	0.30	0.01	0.05	0.14	0.21	-0.00	0.01
	-0.00	0.44	0.19	0.37	0.12	0.22	0.16	0.22	-0.11	0.08	-0.07	0.05	-0.00	0.18	0.00	0.00	0.01	0.01
2.06	0.16	0.56	0.03	0.40	0.14	0.27	-0.01	0.22	0.12	0.10	-0.14	0.31	0.03	0.05	0.11	0.26	-0.00	0.01
	-0.01	0.41	0.21	0.38	0.12	0.24	0.16	0.23	-0.10	0.08	-0.08	0.06	-0.04	0.17	0.01	0.01	0.01	0.02
2.08	0.15	0.55	0.03	0.39	0.13	0.28	-0.00	0.23	0.12	0.11	-0.14	0.32	0.01	0.05	0.06	0.29	-0.00	0.01
	-0.01	0.39	0.22	0.38	0.11	0.25	0.15	0.24	-0.09	0.08	-0.09	0.07	-0.07	0.15	0.02	0.02	0.01	0.02
2.10	0.13	0.54	0.05	0.38	0.12	0.30	0.00	0.23	0.12	0.12	-0.14	0.34	0.03	0.06	0.01	0.31	-0.00	0.01
	-0.02	0.37	0.23	0.39	0.10	0.26	0.14	0.24	-0.08	0.08	-0.09	0.09	-0.08	0.13	0.04	0.03	0.01	0.02
2.12	0.12	0.52	0.06	0.37	0.11	0.31	0.01	0.24	0.12	0.12	-0.14	0.35	0.03	0.06	-0.04	0.30	-0.00	0.01
	-0.02	0.35	0.24	0.40	0.09	0.27	0.13	0.26	-0.07	0.08	-0.09	0.11	-0.09	0.11	0.05	0.04	0.01	0.02
2.14	0.10	0.51	0.08	0.36	0.10	0.32	0.01	0.25	0.11	0.13	-0.15	0.36	0.03	0.06	-0.08	0.29	-0.00	0.01
	-0.02	0.34	0.24	0.41	0.07	0.28	0.11	0.27	-0.07	0.08	-0.09	0.13	-0.09	0.10	0.06	0.06	0.02	0.02
2.16	0.08	0.49	0.10	0.36	0.08	0.33	0.01	0.25	0.11	0.13	-0.16	0.37	0.03	0.07	-0.10	0.27	-0.01	0.02
	-0.01	0.32	0.25	0.42	0.06	0.29	0.09	0.27	-0.06	0.08	-0.09	0.15	-0.09	0.08	0.07	0.07	0.02	0.03
2.18	0.06	0.47	0.12	0.36	0.06	0.33	0.01	0.26	0.10	0.14	-0.17	0.38	0.03	0.07	-0.12	0.25	-0.01	0.02
	-0.01	0.31	0.25	0.43	0.03	0.30	0.07	0.28	-0.06	0.08	-0.09	0.17	-0.09	0.07	0.08	0.08	0.02	0.03
2.20	0.04	0.44	0.14	0.36	0.04	0.34	0.01	0.26	0.09	0.14	-0.19	0.40	0.03	0.08	-0.14	0.23	-0.01	0.02
	-0.00	0.30	0.24	0.44	0.00	0.30	0.05	0.28	-0.06	0.08	-0.07	0.20	-0.09	0.06	0.10	0.09	0.02	0.03
2.22	0.02	0.42	0.17	0.37	0.02	0.35	0.01	0.27	0.08	0.14	-0.21	0.41	0.03	0.09	-0.16	0.21	-0.01	0.02
	0.00	0.29	0.24	0.47	-0.03	0.31	0.02	0.29	-0.05	0.08	-0.06	0.23	-0.08	0.05	0.11	0.10	0.02	0.03

$G_{07}(2100)$: this resonance is well established, however, there is a considerable amount of disagreement with respect to its total width and resonant amplitude, especially in the $\bar{K}N$ channel. The reported total widths range from 60 MeV found in the $\Sigma\pi$ channel [18] to 313 MeV found in $\bar{K}N$ [19]. We consistently found a width of ~ 240 MeV throughout all attempts of fitting. Also the resonant amplitude of 0.31 remained fairly stable in all fits.

$F_{17}(2030)$: this resonance is rather consistently described in $\bar{K}N$, $\Lambda\pi$, and $\Sigma\pi$. The main discrepancies arise from fits to total and partial cross sections. The present analysis yields a width of 172 MeV, in good agreement with the $\Lambda\pi$ and $\Sigma\pi$ analyses, and gives an elastic amplitude of 0.18.

$F_{15}(1915)$: this analysis yields a mass and width comparable with other determinations. The resonant amplitude of 0.11 again contrasts to much lower values obtained in total cross-section fits. This probably reflects a systematic effect in iso-

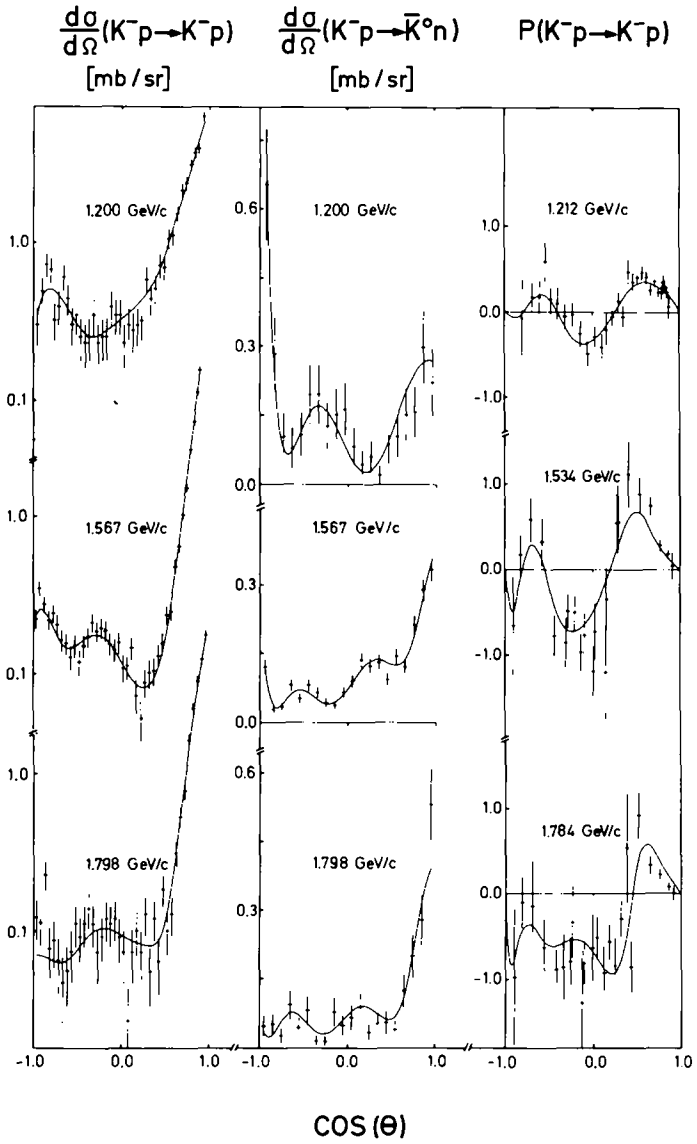

Fig. 5. The measured differential cross section for $K^- p \to K^0 p$, $\bar{K}^0 n$ at 1.2, 1.567 and 1.798 GeV/c from this experiment together with neighbouring polarisation data at 1.212, 1.534 and 1.784 GeV/c [12]. The superposed curves represent solution B.

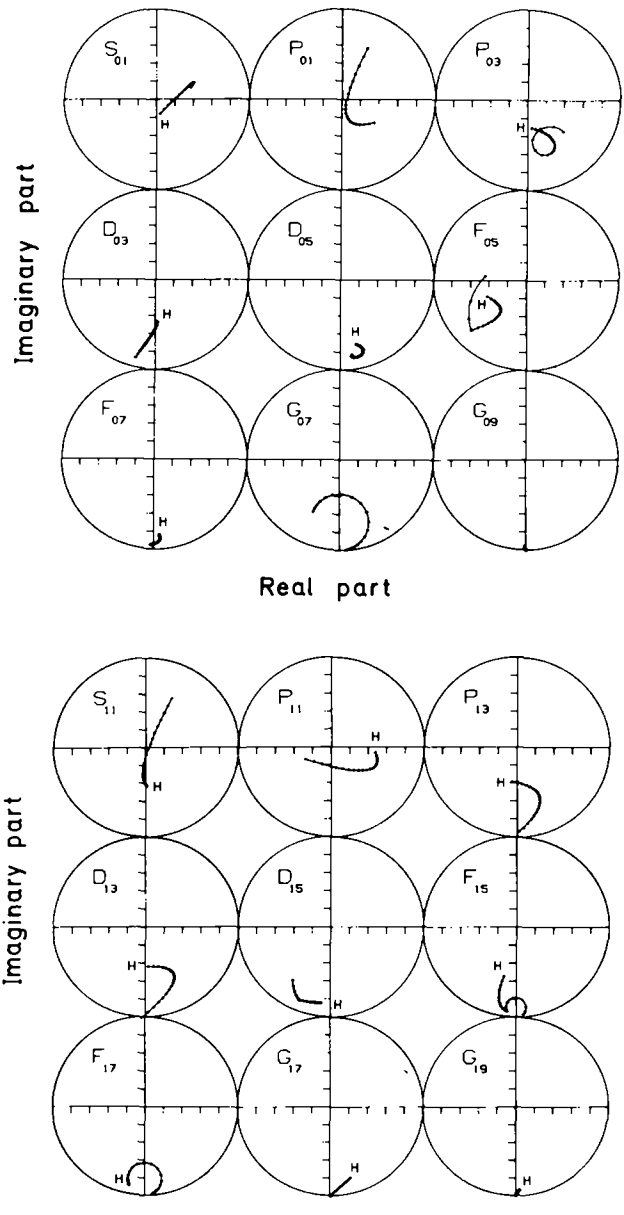

Fig. 6. Argand diagrams for the partial wave amplitudes of solution B. The circles represent the unitary limit for elastic amplitudes (radius = $\frac{1}{2}$; centre at $(0, \frac{1}{2}i)$). The letter H denotes the upper end of the c.m. energy range. The dots represent steps of 20 MeV in the c.m. energy.

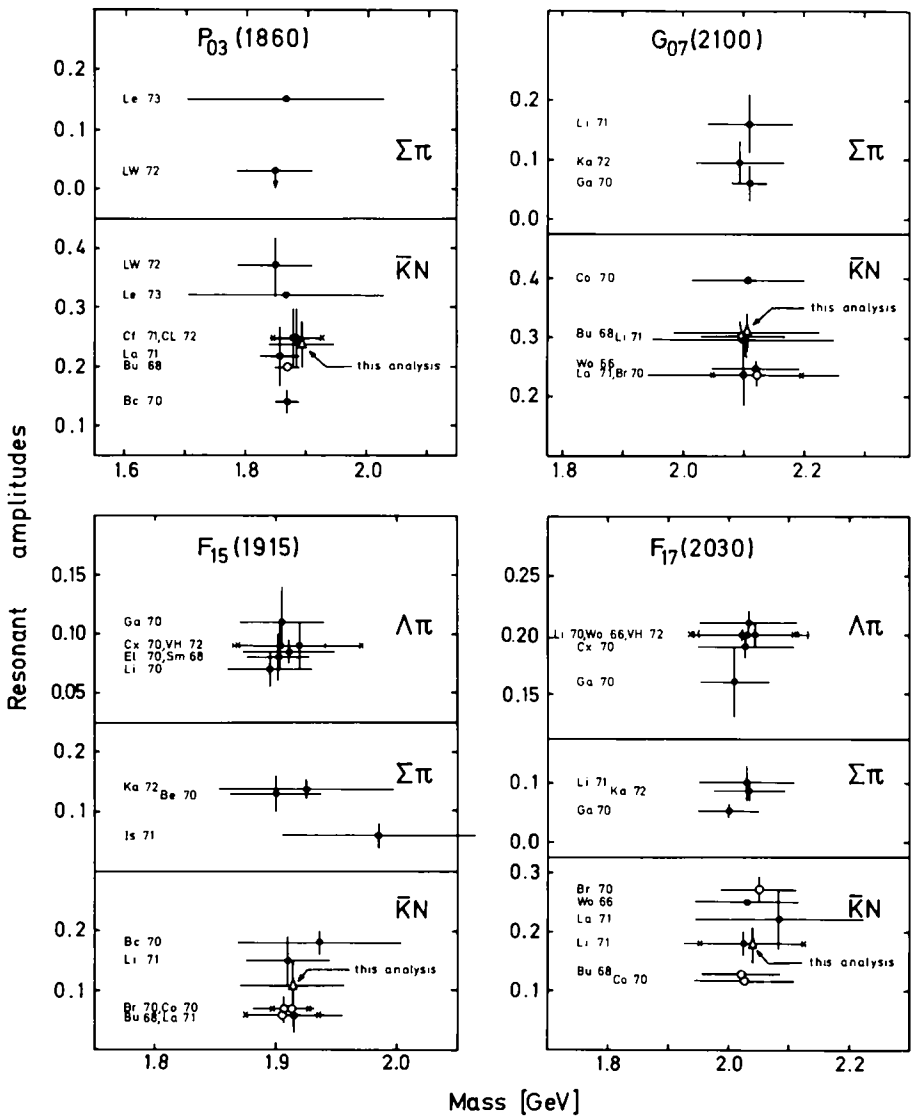

Fig. 7. Compilation of resonance parameters for the $P_{03}(1860)$, $G_{07}(2100)$, $F_{15}(1915)$ and $F_{17}(2030)$. The horizontal bars represent the total width and the vertical bars denote the error on the resonant amplitude. Solid circles refer to partial wave analyses, open circles to results obtained from cross section measurements. The data are taken from the references listed under [17].

lating the $I = 1$ resonant amplitude in the latter analyses, an effect also noticeable for the $F_{17}(2030)$ (see above).

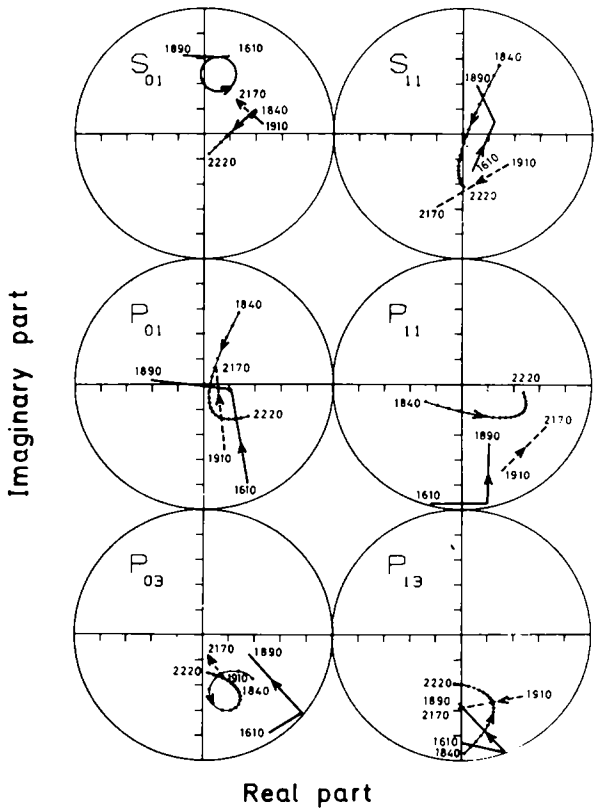

Fig. 8. Argand diagrams for S- and P-waves from this analysis in comparison with those of Litchfield et al. [4] (dashed curve) between 1910 and 2170 MeV and those of Armenteros et al. [22] (solid curve) between 1610 and 1890 MeV. The dots represent steps of 20 MeV in the c.m. energy.

$P_{03}(1860)$: the present analysis adds further confirmation of this $I = 0$ resonance and is in fair agreement with findings in other phase-shift analyses with the exception of [20] and [21]. The resonance remains to be confirmed also in the $\Sigma\pi$ channel, where only weak indications are observed (see fig. 7).

4.2. Continuity of amplitudes

Fig. 8 displays the Argand diagrams for the S and P waves from this analysis. For comparison we also show the amplitudes of Litchfield et al. [4] (dashed curve) within the energy range investigated in this analysis and those of Armenteros et al. [22] (solid curve) whose analysis covers the energy range below 1890 MeV. Poor continuity is observed in all these waves. We find that the discontinuity between the lower energy amplitudes from the present analysis and those of [22] are no larger

than the discrepancies among different sets of solutions at lower energy [23]. Furthermore, neither the analysis of [4] nor the present analysis claim to have found a unique set of S and P wave amplitudes. We feel that the only way to achieve continuity would be to extend the energy range covered by this analysis to lower energies, including measurements of polarisation and Re $f(0)$/Im $f(0)$ which were not available for all earlier analyses. In contrast, all higher partial waves agree well among the relevant analyses.

4.3. A possible F_{07} State at 2100 MeV

Evidence for an F_{07} resonance in the elastic channel was reported by Litchfield et al. [4]. However, it was pointed out that the need for the F_{07} resonance rested solely on a possibly inconsistent polarisation measurement at 1.784 GeV/c. The only other evidence for an F_{07} state, with a reported mass of 2020 ± 20 MeV, comes from an analysis of the $\Sigma\pi$ channel [18]. The data of our analysis do not require an F_{07} resonance. Its addition yields the parameters E_R = 2116 MeV, Γ = 148 MeV, t = 0.04. We feel, however, that resonant structures with amplitudes below 0.05 are out of reach of analyses based on the present data.

4.4. A Possible D_{13} State at 1940 MeV

A recent analysis of the reactions $K^- p \to \Lambda(1520)\pi$ and $K^- p \to \bar{K}\Delta(1230)$ from this experiment [24] has confirmed previous evidence for a resonant structure of the D_{13} wave in the 1940 MeV region. Our analysis does not require a resonant structure in this amplitude. The addition of a D_{13} resonance of mass 1940 MeV and width 80 MeV yields an amplitude of 0.01. If the width is taken as 200 MeV, the amplitude increases to 0.03.

4.5. A resonance of spin-parity $\frac{7}{2}^-$ claimed at 1930 MeV

Dado et al. [6] have claimed in analysis of the elastic $K^- p$ reaction the existence of a further resonant state with unknown isospin and spin-parity $\frac{7}{2}^-$ at 1930 MeV. The quoted resonant amplitude of ~0.6 would produce a bump in the total cross section of ~15 mb which is not observed.

4.6. Bump in the I = 1 total cross section at 2250 MeV

Parameterisations of total cross section data [10] have suggested high mass bumps at ~2350 MeV in the I = 0 channel and at ~2250 MeV in the I = 1 channel. The I = 0 bump is too far above our energy region; however, the effect of the I = 1 bump should be noticeable. While we are not in a favourable position to make a J^P discrimination for this bump, we remark that the only high partial wave from our analysis with sufficient amplitude at 2250 MeV to be consistent with the σ_{tot} data is G_{17}.

References

[1] CERN-Heidelberg-München-Saclay Collaboration, $K^- p$ cross section from 1.136 to 1.434 GeV/c, to be published.

[2] CERN-Heidelberg Collaboration, $K^- p$ cross sections from 1.424 to 1.798 GeV/c, to be published.

[3] R. Armenteros, M. Ferro-Luzzi, D.W.G.S. Leith, R. Levi-Setti, A. Minten, R.D. Tripp, H. Filthuth, V. Hepp, E. Kluge, H. Schneider, R. Barloutaud, P. Granet, J. Meyer and J.P. Porte, Nucl. Phys. B8 (1968) 233;
R. Armenteros, P. Baillon, C. Bricman, M. Ferro-Luzzi, E. Pagiola, J.O. Petersen, D.E. Plane N. Schmitz, E. Burkhardt, H. Filthuth, E. Kluge, H. Oberlack, R.R. Ross, R. Barloutaud, P. Granet, J. Meyer, J.P. Porte and J. Prevost, Nucl. Phys. B21 (1970) 15.

[4] P.J. Litchfield, T.C. Bacon, I. Butterworth, J.R. Smith, E.Lesquoy, R. Strub, A. Berthon, J. Vrana, J. Meyer, E. Pauli, B. Tallini and J. Zatz, Nucl. Phys. B30 (1971) 125.

[5] B. Conforto, D.M. Harmsen, T. Lasinski, R. Levi-Setti, M. Raymund, E. Burkhardt, H. Filthuth, S. Klein, H. Oberlack and H. Schleich, Nucl. Phys. B34 (1971) 41.

[6] S. Dado, A. Birman, J. Goldberg and H. Weiss, Phys. Rev. Letters 29 (1972) 1695; Internal note, $K^- p$ elastic scattering between 1935 and 1990 MeV, Dept. of Physics, Technion, Haifa.

[7] At 1.102, 1.117, 1.134, 1.153, 1.174, 1.183, 1.226 GeV/c:
B. Conforto et al., see [5].
At 1.330 GeV/c:
W.P. Trower, J.R. Ficenec, R.I. Hulsizer, J. Lathrop, J.N. Snyder and W.P. Swanson, Phys. Rev. 170 (1968) 1207.
At 1.22 , 1.42, 1.51, 1.60, 1.70, 1.80, 1.95 GeV/c:
G. Lynch, LBL Berkeley, private communication.
At 1.263, 1.316, 1.368, 1.415, 1.465, 1.513, 1.545, 1.606, 1.652, 1.705, 1.739, 1.800, 1.843 GeV/c:
P.J. Litchfield et al., see [4].
At 1.423, 1.530, 1.680, 1.815 GeV/c:
K. Abe, B.A. Barnett, J.H. Goldman, A.T. Laasanen, P.H. Steinberg, G.J. Marmer, D.R. Moffett and E.F. Parker, Baryon resonances - 73, Purdue University p. 305;
K. Abe, University of Maryland technical report No. 73–056.
At 1.740, 1.772, 1.808, 1.844, 1.880, 1.915, 1.950, 1.990 GeV/c:
P.C. Barber, T.A. Broome, W. Busza, B.G. Duff, D.A. Garbutt, F.F. Heymann, D.C. Imrie, G.J. Lush, E.N. Mgbenu, K.M. Potter, D.M. Ritson, L.A. Robbins, S.J. Sharrock, A.D. Smith, R.C. Hanna, R.A. Rosner and E.J. Sacharides, Conf. on hyperon resonances, Duke University, 1970 (Moore, Durham, 1970) 223.
At 1.305, 1.336, 1.367, 1.396, 1.434 GeV/c:
S. Dado et al., see [6].
At 1.383, 1.433, 1.483, 1.534, 1.584, 1.634, 1.684, 1.734, 1.784, 1.884, 1.934 GeV/c:
C. Daum, F.C. Erné, J.P. Lagnaux, J.C. Sens, M. Steuer and F. Udo, Nucl. Phys. B6 (1968) 273.
At 1.142, 1.212, 1.282, 1.732 GeV/c:
S. Andersson-Almehed, C. Daum, F.C. Erne, J.P. Lagnaux, J.C. Sens and F. Udo, Nucl. Phys. B21 (1970) 515.
At 1.177, 1.250, 1.330 GeV/c:
M.G. Albrow, S. Andersson-Almehed, B. Bosnjakovic, F.C. Erne, Y. Kimura, J.P. Lagnaux, J.C. Sens and F. Udo, Nucl. Phys. B29 (1971) 414.

[8] At 1.102, 1.117, 1.134, 1.153, 1.174, 1.183, 1.226 GeV/c:
R. Armenteros et al., see [3].

At 1.12, 1.42, 1.51, 1.60, 1.70 GeV/c:
C.G. Wohl, Thesis UCRL-16288 (1965).
At 1.80, 1.95 GeV/c:
P.M. Dauber, Thesis UCLA-90024 (1966).
At 1.112, 1.153, 1.192, 1.270, 1.310, 1.345, 1.384, 1.453, 1.500, 1.567, 1.644, 1.694 GeV/c:
A.J. Van Horn, R.P. Ely and J. Louie, Phys. Rev. D6 (1972) 1275.
At 1.263, 1.316, 1.368, 1.415, 1.465, 1.513, 1.545, 1.606, 1.652, 1.705, 1.739, 1.800, 1.843 GeV/c:
P.J. Litchfield et al., see [4].
At 1.330 GeV/c:
W.P. Trower et al., see [7].

[9] C. Bricman, M. Ferro-Luzzi, J.-M. Perreau, G. Bizard, Y. Déclais, J. Duchon, J. Séguinot and G. Valladas, Phys. Letters 31B (1970) 148;
C. Bricman, CERN/D.Ph. II/PHYS 72-29.

[10] R.L. Cool, G. Giacomelli, T.F. Kycia, B.A. Leontic, K.K. Li, A. Lundby, J. Teiger and C. Wilkin, Phys. Rev. D1 (1970) 1887;
D.V. Bugg, R.S. Gilmore, K.M. Knight, D.C. Salter, G.H. Stafford, E.J.N. Wilson, J.D. Davies, J.D. Dowell, P.M. Hattersley, R.J. Homer, A.W. O'Dell, A.A. Carter, R.J. Tapper and K.F. Riley, Phys. Rev. 168 (1968) 1466.

[11] P. Baillon, C. Bricman, M. Ferro-Luzzi, J.-M. Perreau, R.D. Tripp, T. Ypsilantis, Y. Declais and J. Séguinot, Phys. Letters 50B (1974) 383.

[12] At 1.11, 1.14, 1.16, 1.28, 1.31, 1.34, 1.37 GeV/c:
C.R. Cox, P.J. Duke, K.S. Heard, R.E. Hill, W.R. Holley, D.P. Jones, F.C. Shoemaker, J.J. Thresher, J.B. Warren and J.C. Sleeman, Phys. Rev. 184 (1969) 1443.
At 1.383, 1.433, 1.483, 1.534, 1.584, 1.634, 1.684, 1.734, 1.784, 1.884, 1.934, 1.984 GeV/c:
C. Daum et al., see [7].
At 1.142, 1.212, 1.282, 1.732 GeV/c:
S. Andersson-Almehed et al., see [7].
At 1.177, 1.250, 1.330 GeV/c:
M.G. Albrow et al., see [7].
At 1.830, 1.940 GeV/c:
M.E. Zeller, Yale Univ., private communication.

[13] G. Lynch, Conf. on hyperon resonances, Duke university, 1970 (Moore, Durham, 1970) 9.

[14] P. Baillon, C. Bricman, M. Ferro-Luzzi, J.-M. Perreau, R.D. Tripp, T. Ypsilantis, Y. Déclais and J. Séguinot, Phys. Letters 50B (1974) 377.

[15] J.M. Blatt and V.F. Weisskopf, Theoretical nuclear physics, (Wiley New York, 1952).

[16] T.A. Lasinski, A. Barbaro-Galtieri, R.L. Kelly, A. Rittenberg, A.H. Rosenfeld, T.G. Trippe, N. Barash-Schmidt, C. Bricman, V. Chaloupka, P. Söding and M. Roos, Rev. Mod. Phys. 45 (1973).

[17] Wo66: C.G. Wohl, F.T. Solmitz and M.L. Stevenson, Phys. Rev. Letters 17 (1966) 107.
Bu68: see [10].
Sm68: W.M. Smart, Phys. Rev. 169 (1968) 1330.
Bc70: see [20].
Be70: A. Berthon, J. Vrana, I. Butterworth, P.J. Litchfield, J.R. Smith, J. Meyer, E. Pauli and B. Tallini, Nucl. Phys. B24 (1970) 417.
Br70: C. Bricman, M. Ferro-Luzzi, J.-M. Perreau, G. Bizard, Y. Déclais, J. Duchon, J. Séguinot and G. Valladas, Phys. Letters 31B (1970) 152.
Co70: see [10].
Cx70: G.F. Cox, G.S. Islam, D.C. Colley, D. Eastwood, J.R. Fry, F.R. Heathcote, D.J.

Candlin, J.G. Colvine, G. Copley, N.E. Fancey, J. Muir, W. Angus, J.R. Campbell, W.T. Morton, P.J. Negus, S.S. Ali, I. Butterworth, F. Fuchs, D.P. Goyal, D.B. Miller, D. Pearce and B. Schwarzschild, Nucl. Phys. B19 (1970) 61.
E170: R.P. Ely, Jr., R.W. Birge, J. Hoven, G.E. Kalmus, D. Kane and A. Van Horn, UCRL-19789 15th Int. Conf. on high-energy Physics, Kiev, 1970.
Ga70: see [18].
Li70: P.J. Litchfield, Nucl. Phys. B22 (1970) 269.
Cf71: see [5].
Is71: G.S. Islam, G.F. Cox, D.C. Colley and F.R. Heathcote, Pakistan, J. Sci. Ind. Res. 14 (1971) 305.
La71: see [19]; Li71: see [4].
CL72: Chicago-LBL Collaboration, 16th Int. Conf. on high-energy physics, Chicago, 1972.
Ka72: D.F. Kane, Jr., Phys. Rev. D5 (1972) 1583.
LW72: see [21].
VH72: A.J. Van Horn, Ph. D. thesis, LBL-1370 (1972).
Le73: A.T. Lea, B.R. Martin, R.G. Moorhouse and G.C. Oades, Nucl. Phys. B56 (1973) 77.

[18] A. Barbaro-Galtieri, Conf. on hyperon resonances, Duke University, 1970 (Moore, Durham, 1970) 173.

[19] T.A. Lasinski, Nucl. Phys. B29 (1971) 125.

[20] C. Bricman, M. Ferro-Luzzi and J.P. Lagnaux, Phys. Letters 33B (1970) 511.

[21] W. Langbein and F. Wagner, Nucl. Phys. B47 (1972) 477.

[22] R. Armenteros, P. Baillon, C. Bricman, M. Ferro-Luzzi, D.E. Plane, N. Schmitz, E. Burkhardt, H. Filthuth, E. Kluge, H. Oberlack, R.R. Ross, R. Barloutaud, P. Granet, J. Meyer, J.P. Porte and J. Prevost, Nucl. Phys. B8 (1968) 195.

[23] R. Armenteros, M. Ferro-Luzzi, D.W.G. Leith, R. Levi-Setti, A. Minten, R.D. Tripp, H. Filthuth, V. Hepp, E. Kluge, H. Schneider, R. Barloutaud, P. Granet, J. Meyer and J.P. Porte, Nucl. Phys. B3 (1967) 592;
R. Armenteros et al., see [22];
B. Conforto, D.-M. Harmsen, T. Lasinski, R. Levi-Setti, M. Raymund, E. Burkhardt, H. Filthuth, E. Kluge, H. Oberlack and R.R. Ross, Nucl. Phys. B8 (1968) 165;
D.S. Bailey, UCRL-50617 (1969);
R. Armenteros, P. Baillon, C. Bricman, M. Ferro-Luzzi, E. Pagiola, J.O. Petersen, D.E. Plane, E. Burkhardt, H. Filthuth, E. Kluge and H. Oberlack, Conf. on hyperon resonances, Duke University, 1970 (Moore, Durham, 1970) 123;
C. Bricman et al., see [20];
B. Conforto et al., see [5];
J.K. Kim, Phys. Rev. Letters 27 (1971) 356;
T.A. Lasinski, see [19];
Chicago LBL Collaboration, see [17];
W. Langbein et al., see [21];
A.T. Lea et al., see [17].

[24] P.J. Litchfield, R.J. Hemingway, P. Baillon, A. Putzer and H. Schleich, Nucl. Phys. B74 (1974) 19.
P.J. Litchfield, R.J. Hemingway, P. Baillon, A. Albrecht and A. Putzer, Nucl. Phys. B74 (1974) 39.